DIFFRACTION PHENOMENA:

REVIEW OF THE EXPERIMENTAL SITUATION

David W. G. S. Leith
Stanford Linear Accelerator Center, Stanford University
Stanford, California 94305 (USA)

Introduction:

This talk is intended to be a general introduction to what we believe we know about the diffraction phenomena and, by inference, the Pomeron. The phenomena is important in many fields of physics and appears to be well understood in optics and nuclear physics experiments. An example is given in Fig. 1, where the angular distribution for α-particle scattering on Fe^{58} at 64 MeV is shown, in which the Rutherford scattering contribution has been divided out from the measured cross section.[1] The data show a clear and impressive series of diffraction maxima and minima. In high energy particle physics diffraction is also an important phenomena, accounting for ~ 30% of the total cross section, but it is not well understood. We describe diffraction in terms of two pictures -- one a geometrical model in which we discuss the scattering of particles on an absorbing disc of a given size and with a given opacity

(sometimes with edge effects taken into account) and the other a t-channel dynamical picture where we talk of particle exchange between the incident particle and the target particle (viz. Regge theory and its modifications). The exchanged particle in the case of diffraction processes is called the Pomeron. In Regge theory the energy dependence of the cross section is controlled by the trajectory properties of the exchanged particle

$$\sigma(S) \propto S^{\alpha(0)-1}.$$

Thus the flat total cross sections expected from a diffractive process are accounted for by the exchange of Pomeron with a trajectory given by

$$\alpha(0) = 1.$$

The Pomeron has quite an unusual role in particle physics, in that

-- no other pole has a trajectory with $\alpha(0)=1$;

-- there is no known particle to be associated with this trajectory, (i.e. unusual behaviour of the trajectory for $t > 0$);

-- the behaviour of the trajectory for $t < 0$, as seen in the shrinkage of the differential cross section,

$$\frac{d\sigma}{dt}(s,t) \propto S^{2\alpha(t)-2}$$

is quite different from other trajectories. The Pomeron trajectory has a rather flat t-dependence, $\alpha(t) = 1+\alpha' t$ with $0 < \alpha' < \cdot 4$ GeV^2 while other known trajectories have $\alpha' \sim 1$ GeV^2;

-- the particle behaves in scattering processes as though it carried the quantum numbers of the vacuum, whereas it behaves with respect to cross sections like a particle with spin 1.

The processes from which we learn about diffraction and the properties of the Pomeron are

(a) $A + B \to A + B$ -- the elastic scattering reaction, which is related to the total cross section through the optical theorem;

(b) $\left.\begin{matrix} A + B \to A^* + B \\ A + B^* \end{matrix}\right\}$ - inelastic scattering, in which the projectile or target is excited -- diffraction dissociation. This process was discussed by Good and Walker[2] in analogy to optical diffraction by an opaque disc. They predicted that such processes would occur, that they would proceed coherently in nucleii, and that the scattering properties would be very similar to those of the elastic reaction.

(c) $\left.\begin{matrix} A + B \to A + X \\ X + B \end{matrix}\right\}$ - inelastic, inclusive scattering. This process becomes of considerable interest at high energies.

Unfortunately, we do not have a good description of the diffraction process in particle physics, or of the Pomeron. Basically what we do have is a set of rules that allow us to identify what we mean by diffractive reaction or Pomeron exchange processes.

These rules are listed below.

-- energy independent cross sections (to factors of log S)

-- sharp forward peak in $d\sigma/dt$

-- particle cross sections equal to anti-particle cross sections

-- factorization

-- mainly imaginary amplitude

-- exchange processes characterized by the quantum numbers of the vacuum in the t-channel (i.e. I = 0, C = +1). Also, the change in parity in the scattering process follows the natural spin-parity series $(-1)^J$, or

$$P_f = P_i \cdot (-1)^{\Delta J},$$ where ΔJ is spin change.

-- the spin structure in the scattering is s-channel helicity conserving, (SCHC).

We will proceed to examine how well these rules are obeyed.

Cross Sections:

The energy dependence of total cross sections have been described in terms of two components -- a diffractive component associated with the exchange of a Pomeron, and a second component due to the exchange of other Regge trajectories. The Pomeron term gave rise to a flat contribution to the cross section, while the Regge part fell like a power of the energy. These ideas worked well for the data up to about 25 GeV/c, but do not work so well for the new data covering energies up to 70 GeV from Serpukov.

In Fig. 2 the total cross sections for $\bar{p}p$, pp, $\pi^{\pm}p$ and $K^{\pm}p$ are shown from a few GeV up through the Serpukov energy region. The data[3] may be summarized as follows:

-- $\pi^{\pm}p$, $K^{-}p$, $K^{-}n$, pp, pn total cross sections seem to have reached a plateau with little or no energy dependence;

-- $\bar{p}p$ and $\bar{p}n$ total cross sections are decreasing;

-- $K^{+}p$, $K^{+}n$ are increasing with energy in the region from 20 to 60 GeV/c;

-- the difference between Xp and $\bar{X}p$ is decreasing with energy and fits[4]

$$\Delta\sigma \propto A p_{lab}^{-n}$$

where n is given in Table 1;

-- Λp, Λn total cross sections are flat in the region (6-21) GeV/c;

-- γp, γn total cross sections have been measured up to 30 GeV. The S-dependence is very similar to that of

πN scattering. They find

$$\sigma(\gamma p) = A + Bp^{-1/2} = (97.4 \pm 1.9) + (55 \pm 5)_f E^{-1/2} + (12 \pm 2.5)_{A_2} E^{-1/2}$$

where the determination of the isoscalar (f) and isovector contributions come from comparison of the γp and γn rates;

-- The Okun-Pomeranchuk theorem, which states that the cross-sections of particles belonging to the same isospin multiplet should become equal as the energy goes to infinity, seems to be close to satisfied.

-- The Pomeranchuk theorem, which states that particle and anti-particle cross sections should be the same at asymptotic energies, seems also to be becoming satisfied. The difference in cross sections are falling as a power of the energy (see Table I) and should soon approach zero.

The situation for the pp total cross section has changed over the last few months in a very exciting way. The preliminary ISR data, and the NAL bubble chamber cross section measurements presented at Batavia[3] had large statistical and systematic errors and were quite consistent with a flat pp total cross section of 38 mb extrapolated up from the Serpukov energy region. There were, however, some indications from cosmic ray studies that the pp cross section increased at high energies, maybe even in the ISR energy region.[5]

New data from two ISR groups now show good evidence for such a rising pp total cross section, see Fig. 3. The measurements come from two very different techniques; the Bellettini group[6] measure the total cross section by counting the secondary products while the Cocconi group[7] find the total cross section by measuring the forward elastic cross section and applying the optical theorem. They measure the real part of the pp scattering amplitude at several energies to show that it is small at these energies and that its effects are negligible.

Both experiments rely heavily on measurement of the luminosity of the ISR (i.e. the number of colliding protons in the two rings per unit area). Great care has been taken in arriving at estimates of the luminosity and several different techniques for measuring it employed. Some agreement between the different methods seems to be obtained and the luminosity is claimed to be known to ~ 1-2%.

The results of the experiments agree well and show ~ 4 mb increase in the p-p cross section between (300 and 1500) GeV/c equivalent lab momentum. This observation raises many interesting questions; for example, how should we now think of asymptopia? Will the total cross section continue to rise indefinitely or will it approach an asymptotically flat cross section from below? Is the rise due to an expanding radius of the proton as the energy increases or is it due to some negative interference effect whose magnitude decreases with energy? What sets the scale for the onset of the increase; i.e. K^+p starts increasing around 20 GeV/c, p-p at

200 GeV/c -- when do $\pi^{\pm}p$, $K^{-}p$ and γp start increasing? Whatever the answers to these questions may be, and it will be a long time before we know them all, one thing is clear -- the model of a simple pole (the Pomeron) describing the high energy scattering behaviour is not going to work.

One amusing thought comes to mind -- after all these years of worrying about the $\bar{p}p$ total cross section falling with increasing energy, to meet the pp value to satisfy the Pomeranchuk theorem, we now see that it will have to turn around and also start increasing in order to catch up (or keep up) with the high energy pp cross section.

Further data on the energy dependence of cross sections for processes expected to be dominated by the diffraction phenomena are shown in Figs. 4 and 5, where the pp,[8] and $\pi^{-}p$, $K^{-}p$, and $\bar{p}p$[9] elastic cross sections are, respectively, plotted versus laboratory momentum. The characteristic flattening of the cross section as the energy increases is observed in each case. The momentum dependence of several total and elastic cross sections is given in Table 2.

The ratio of elastic to the total cross section, σ_{el}/σ_{tot}, is of interest under the assumption that we are dealing with diffraction and a geometrical picture. We have

$$\frac{\sigma_{el}}{\sigma_T} = \frac{\sigma_T^2}{\sigma_T \cdot b} = \frac{\sigma_T}{b} \propto \frac{(\text{Radius})^2}{(\text{Radius})^2} = \text{constant.}$$

i.e. at high energy one expects this ratio to be constant, and the same for particle and anti particle. Table 3 summarises data on particle-anti particle cross section ratios. It is rather incon-

clusive due to the lack of data at high energy. The one system where good data is available is for p-p scattering. Fig. 6 shows the ratio σ_{el}/σ_{tot}, for pp scattering from (1-2000) GeV/c, and demonstrates that for $p_{lab} \gtrsim 60$ GeV/c the ratio is indeed constant. This is specially interesting in the (200-1500) GeV/c region where the total cross section rises by ~ 10%; the elastic cross section increases by the same amount and the ratio stays flat.

Another interesting property of elastic scattering cross section is summarized in Table 4, where the ratios of particle to anti particle cross section are listed. It is surprising the extent to which the equality seems to be preserved, even at energies where one knows that Regge exchange process contributes substantially and therefore the process cannot be all Pomeron exchange.

Differential Cross Sections:

Let us now consider how well the "rules" and data on differential cross sections agree. The most interesting data comes from ISR studies of p-p scattering by the Rubbia group. An example of their data[10] is shown in Fig. 7. With high statistics and a precision wire spark chamber spectrometer they have studied elastic p-p scattering from (150-1500) GeV/c equivalent lab momentum.

The angular distribution is sharply forward peaked, but the data clearly show a change in the slope of the differential cross section at small t, in fact the break occurs around t = 0.13 GeV^2. The cross section is not well fit by a single exponential slope,

but fairly well described by two exponentials, e^{-at}, where $a = 12.8\ \text{GeV}^{-2}$ for $0.01 \leq t \leq 0.12\ \text{GeV}^2$, and $a = 10.8\ \text{GeV}^{-2}$ for $0.15 \leq t \leq 0.5\ \text{GeV}^2$. These observations help explain the inconsistencies between older measurements of the slope in p-p scattering cross sections made at lower energy and in different t ranges. It should be noted that this description of the data, in terms of two exponentials, is not unique and that perhaps a more continuous description would be preferable.

The overall picture of the s-dependence of the slope, b, is shown in Fig. 8.[11] The data have been fit to an exponential in two t ranges, $t < 0.1\ \text{GeV}^2$ and $0.15 < t < 0.5\ \text{GeV}^2$, from 1 GeV/c through the ISR range, (~ 2000 GeV/c equivalent lab momentum). The Serpukov data have been lowered by $\Delta b \sim 0.4\ \text{GeV}^{-2}$, which is within their quoted systematic error, and the whole data set above 30 GeV/c fit to

$$b(s,t) = b_o(t) + 2\alpha(t)\ \ell n\ \frac{s}{s_o}\ .$$

The fits are quite good and result in the following parameters:

low t region: $b_o = (7.0 \pm 1.2)$, $\alpha = (0.37 \pm 0.08)$

high t region: $b_o = (9.2 \pm 0.94)$, $\alpha = (0.10 \pm 0.06)$.

In other words, the cross section is made up of a forward region which exhibits substantial shrinkage, and a larger t region which is essentially constant in t.

As an example of other elastic data, $\pi^- p$, $K^- p$ and $\bar{p}p$ scattering cross sections at 25 and 40 GeV/c are shown in Fig. 9.[9] These data show sharp forward peaks, and when fit over the whole t

range measured, (i.e. $0.1 < t < 0.6$ GeV^2), require quadratic terms in t, (e.g. $d\sigma/dt \propto e^{at + bt^2}$).

A summary of the s-dependence of the slope for elastic scattering, as measured at $t \sim 0.2$ GeV^2, is shown in Fig. 10.[11,12] The slopes for particle and for antiparticle scattering seem to become equal at high energies with asymptotic slopes of ~ 8 GeV^{-2} for πN, $\sim 7\text{-}1/2$ GeV^{-2} for KN and ~ 11 GeV^{-2} for NN scattering. The $\pi^- p$ and $K^- p$ data show almost no shrinkage (i.e. no s-dependence of the slope), while the $\bar{p}p$ data show considerable antishrinkage up through the Serpukov region. The $K^+ p$ and p-p data show considerable shrinkage, while the $\pi^+ p$ data also shows shrinkage but much less.

Inelastic Processes; Cross sections

While we are dealing with elastic cross sections, let us consider the same information for the diffractive inelastic processes. A more complete review of this data may be found in the Batavia Conference proceedings.[13] For this discussion we will not try to answer the question of whether these inelastic processes are kinematic in origin or are dominated by resonance production, but merely observe that production of the "A_1 Region" by π's, the "Q Region" by K's and excited N*'s by N's are well defined, clearly identifiable reactions dominated by a single well defined spin-parity state.

The cross sections for these processes are quite flat as a function of energy, characteristic of diffractive processes.

For example, Fig. 11 shows the cross section for the reaction $K_L^o p \to Q^o p$ as a function of energy from (1-1/2 - 12) GeV/c from the SLAC $K^o p$ HBC experiment.[14] The energy dependence of the Q^o production cross section is found to fall as $p_{lab}^{-0.59}$. Table 5 summarizes the information for other inelastic processes and compares them to the elastic data. The inelastic processes seem to fall off a little faster than the corresponding elastic reaction, but it is not clear whether this difference is important or whether it is due to the technical difficulty of determining an "A cross section" or a "Q cross section" above the backgrounds. However, it is clear that these inelastic diffractive processes are much more like the elastic reactions than the typical Regge exchange processes where cross sections fall like $p^{-1.5}$, or faster.

These inelastic reactions also have the property that particle and antiparticle cross sections are equal. We find that:

-- the ratio of $K^o \to Q^o$ to $\overline{K}^o \to \overline{Q}^o$ in the momentum interval (4-12) GeV/c is 0.98 ± 0.08[14]

-- the ratio of $\pi^{\pm} \to A_1^{\pm}$ at 15 GeV/c is 1.00 ± 0.07,[15] 0.94 ± 0.12.[16]

The angular distributions are also sharply peaked in the forward direction with slopes comparable to, but slightly steeper than, the elastic reaction. Whether the 1-2 unit difference between elastic and related inelastic slopes is real and significant or whether it is merely a background problem will not be discussed. What is clear, is that the slopes are comparable to, and that they observe the same relationships between processes as the elastic

reactions (e.g. the slope for $\pi p \to Ap$ is greater than $Kp \to Qp$ which is less than $\bar{K}p \to \bar{Q}p$ just as $\pi p \to \pi p$ is to $Kp \to Kp$, is to $\bar{K}p \to \bar{K}p$). Data on the slope of various inelastic reaction cross sections is summarized in Table 6.

Finally, the inelastic reactions also exhibit the crossover phenomenon in the differential cross sections. The elastic process which is dominated by Pomeron exchange does, however, have some Regge exchange contribution. This additional contribution gives rise to different slopes in the cross section for particle and for antiparticle scattering. An example of this phenomena is shown in Fig. 12, where preliminary 13 GeV/c cross sections for K^+p and K^-p elastic scattering from the SLAC wire spark chamber spectrometer experiment[17] are displayed. A clear cross-over of the differential cross sections is seen for momentum transfers ~ 0.15-0.2 GeV^2. Similar behaviour is observed in $K^0p \to Q^0p$ and $\bar{K}^0p \to \bar{Q}^0p$[14] as seen in Fig. 13. The slope for the strangeness +1 and -1 processes are very similar and the crossover occurs in about the same place.

It is interesting to see how similar the elastic and inelastic (diffractive dissociation) processes are with respect to total cross section and differential cross section behaviour.

Two puzzles:

Although much of the data on angular distributions for elastic and for inelastic processes discussed above agrees well with our list of "rules", and our prejudice for diffractive reactions, there are two outstanding puzzles. (a) If all elastic

scattering reactions are dominated by Pomeron exchange why is the behaviour of the slope of the forward peak as a function of energy so different for different particles -- why does K^+p and pp shrink strongly, π^+p weakly, π^-p and K^-p essentially flat, and $\bar{p}p$ anti-shrink?

This question has been answered for the $\pi^{\pm}p$ system in a very nice analysis by Davier,[18] and for $\gamma p \to \rho^o p$ by Chadwick, Eisenberg, and Kogan.[19] In both analyses the Dual Absorption Model was applied assuming that only the Pomeron and the f^o meson contributed to the iso-scalar t-channel amplitude. The Pomeron was parameterized as a central collision process while the f^o was given a Regge energy dependence and assumed to be peripheral. The data was well fit with this amplitude and the resulting Pomeron contributions showed substantial shrinkage, in good agreement with the K^+p data.

Fig. 14 shows the K^+p slope as a function of energy as the shaded band, and the data points are the Pomeron contribution to $\pi^{\pm}p$ elastic scattering from Davier's analysis. It is interesting to see how well they agree.

Fig. 15 shows the angular distribution of $\gamma p \to \rho p$ at several energies and the fit using the above description. Also shown is the energy dependence of the slope of the Pomeron contribution to this process. Again this agrees well with the Pomeron in πN collisions as derived by Davier and with the K^+p data. It is interesting that the πN and γN data which show practically no shrinkage actually contain a Pomeron contribution which is shrinking

just like the K^+p case.

Thus we see that small admixtures of a non-diffractive amplitude may markedly change the energy dependence of the differential cross section, and that in the two cases studied in detail, the data proved to be consistent with the "same Pomeron" in all the diffractive amplitudes.

(b) We can call this the "ϕ-meson puzzle." The photoproduction of ϕ-mesons is supposed to be our best "laboratory" for studying the properties of diffraction. The ϕ-meson does not couple to hadrons and so the only contribution to the t-channel exchange should be the Pomeron. Therefore, in an unambiguous way we hope to learn of the Pomeron from the reaction $\gamma p \rightarrow \phi p$.

The cross section for this process is shown in Fig. 16, and is flat beyond threshold, or perhaps rises a little.[13] Examples of measurements of the differential cross section are given in Fig. 17[13] and the energy dependence of the slope of the forward peak is given in Fig. 18. The data is consistent with either no shrinkage on one hand, or quite considerable shrinkage if pushed to the other extreme. The Ritson group attempted to settle this question by measuring the s-dependence of the cross section at a particular t-value, $t=0.6$ GeV^2.[20] The results are shown in Fig. 19. If the shrinkage of the differential cross section is analyzed in terms of

$$\alpha(t) = \alpha(0) + \alpha' t$$

their data give $\alpha' = (-0.03 \pm 0.13)$.

This flat energy dependence is just not what we expect for the Pomeron, or at least not what we have learned from K^+p and p-p elastic scattering. One may worry about the large t value at which these measurements were made, and that the amplitude would no longer be diffraction dominated so far from the forward direction. However, in p-p scattering at similar energies quite strong shrinkage is observed at these t-values -- see Fig. 20. So we have a puzzle; what is going on in $\gamma p \to \phi p$?

We do know that the process is diffractive, in that it is almost completely natural parity exchange and that it proceeds coherently on nucleii -

(a) The Ritson group at SLAC have measured the asymmetry parameter in ϕ photoproduction with polarized photons; $\Sigma = \frac{\sigma_{\parallel} - \sigma_{\perp}}{\sigma_{\parallel} + \sigma_{\perp}}$ (with polarization $\parallel$ ($\perp$) to the decay plane of the ϕ). The experiment was performed using a diamond crystal to polarize the photon beam and by detecting both the recoil proton and the K^+K^- decay of the ϕ-meson. They found that $\Sigma = 0.985 \pm 0.12$ at 8 GeV and at $t = 0.2$ GeV^2 which is consistent with complete natural parity exchange.

(b) The above observations are supported by SLAC-Berkeley-Tufts back-scattered laser experiment. They have studied ϕ-photoproduction in the bubble chamber using the polarized photon beam and find that the decay density matrix elements and measured asymmetry at 4.8 and 9.3 GeV are consistent with pure natural parity exchange.

(c) The DESY/MIT group have studied ϕ-photoproduction from a carbon target at around 7 GeV.[24] They observed copious coherent production of the ϕ, and analysis of the decay distribution is again consistent with natural parity exchange.

However, there is one piece of evidence that although the forward $\gamma p \to \phi p$ process may be dominantly natural parity, it may not be purely imaginary as would have been expected for pure Pomeron exchange. The DESY/MIT group have measured the real part of the $\gamma p \to \phi p$ process by observing the interference between the resonant ϕ production and the Bethe-Hietler process in $\gamma C \to \phi C$, with $\phi \to e^+e^-$ at 7 GeV.[25] They report that the ϕ amplitude differs from being purely imaginary by $25^\circ \pm 15^\circ$ or, in other terms, $\left(\frac{\mathrm{ReA}_\phi}{\mathrm{ImA}_\phi}\right) = (-0.48 \pm {}^{.33}_{.45})$. This may be an indication that the $\gamma \to \phi$ process is not purely due to Pomeron exchange. Unfortunately, this is a difficult experiment and the accuracy is not good enough to draw firm conclusions:

To summarize, the ϕ photoproduction experiments provide a puzzling input on the shrinkage properties of the Pomeron. Two possible ways out of the conflict with the K^+p and pp data have been identified -- (a) that $t = 0.6$ GeV^2 is a large t for diffraction dominance and that non-leading effects may be confusing the situation, and (b) that there may be a large real part in $\gamma p \to \phi p$. Whatever the explanation, it is important to redo the Ritson experiment, studying the ϕ cross section as a function of photon energy, but at a much smaller t-value, (e.g. for $t \sim 0.1$ GeV^2).

Factorization:

If we really believed that these diffraction reactions are dominated by the exchange of a simple Pomeron, we should be able to factorize, or separate, the different vertices appearing in these processes.

For example, the three sets of reactions shown in Fig. 21 should have the same ratio independent of the nature of the incident particle. The results of this test are shown in Fig. 22, for two energies, as a function of momentum transfer.[26] Factorization is observed to hold within ~ 20%, and even seems to work as a function of t.

Two further examples of factorization tests on total cross sections are described below:

Consider the process illustrated in Fig. 23 with elastic pion and proton scattering at the upper vertex, and proton diffraction into a proton plus zero, one, two, or three pions at the bottom vertex, the ratio between cross sections of the two upper vertex processes should be the same, independent of which of the four bottom vertices they interact.

$$\text{e.g., } R_1 = \frac{\sigma(\pi p \to \pi p)}{\sigma(pp \to pp)} \text{ should equal } R_2 = \frac{\sigma(\pi p \to \pi(p\pi^o))}{2(pp \to p(p\pi^o))} \text{ etc.}$$

A paper was submitted to the Batavia Conference by the Scandinavian Bubble Chamber Collaboration[27] in which the above diffractive processes have been isolated using the Van Hove Longitudinal Phase Space (LPS) analysis.[28] The results are given in Table 7 and the agreement is surprising.

Another interesting test of factorization in diffractive processes was presented by the SLAC Streamer Chamber Group.[29] The reactions studied are given schematically in Fig. 24, where each of the diffractive contributions -- $\gamma \rightarrow \rho^o$, $\pi \rightarrow \pi$, and $p \rightarrow p$ at the top vertex, and $p \rightarrow p$ and $p \rightarrow (p\pi\pi)$ at the bottom vertex -- were isolated using the LPS analysis. If the Pomeron contribution were well behaved and factorizable, then we would expect the ratio of the cross sections for each of the top vertex process joined to both of the bottom vertex processes, to be equal. For example, we would expect $R_1 = R_2 = R_3$, where

$$R_1 = \frac{\sigma(\gamma p \rightarrow \rho^o p)}{\sigma(\gamma p \rightarrow \rho^o(p\pi\pi))}$$

and

$$R_2 = \frac{\sigma(pp \rightarrow pp)}{\sigma(pp \rightarrow p(p\pi\pi))} \quad , \qquad R_3^{\pm} = \frac{\sigma(\pi^{\pm} p \rightarrow \pi^{\pm} p)}{\sigma(\pi^{\pm} p \rightarrow \pi^{\pm}(p\pi\pi))}$$

The experimental values for R_1, R_2, and R_3 are given in Table 8 for three different energy regions. Again the agreement is surprisingly good.

In summary, the factorization assumption for diffractive processes seems to be good to $\sim$ 15-20%. It would be interesting to have some more precise tests in the (10-20) GeV/c region, to look for the breaking of the assumption that one might expect from the presence of non-leading effects, like cuts.

Quantum Numbers in Pomeron Exchange:

The "rules" for diffractive processes said that, from a t-channel point of view, the Pomeron would carry the quantum numbers of the vacuum (i.e. C = +1, I = 0 exchange). How well does the data support this assertion?

(a) I = 0 Character:

We know from amplitude analysis of elastic scattering (which we suppose to be mainly diffractive) that the dominant amplitude is the non-flip isoscalar t-channel amplitude. We also know that processes involving a change of charge in the scattering (and hence $I \neq 0$ in the t-channel) have cross sections which fall quite rapidly with energy and do not have the character of diffractive reactions.

Below we consider two examples of the I = 0 character of diffractive processes from inelastic scattering:

The reactions $\pi^- p \to N\pi\pi$ were studied at 16 GeV/c by the ABBCCHW collaboration[26] and the $N\pi$ mass spectra are shown for the various possible charge combinations (see Fig. 25). The $(N\pi)^+$ combinations, (i.e. $p\pi^0$, $n\pi^+$) which can be produced with no charge exchange and hence accessible from I = 0 exchange in the t-channel, exhibit a large low mass enhancement in the (1400-1700) MeV range. This enhancement has an almost energy-independent cross section and is related to the diffractive excitation of N^*'s. The $(N\pi)^0$ combinations (i.e. $p\pi^-$, and $n\pi^-$ respectively), which cannot be reached with I = 0 exchange, have no low mass diffractive enhancement.

A similar example is shown in Fig. 26, where 10 GeV/c $K^- p \to \overline{K}(N\pi\pi)$ reactions have been studied.[26] Again the $(N\pi\pi)^+$ mass spectrum shows a low mass enhancement associated with the diffractive production of excited N^*, while the $(N\pi\pi)^0$ spectrum shows no such structure.

Thus we see quite clearly that the observation of diffractive phenomena is closely connected with I = 0 in the t-channel.

(b) C = +1 Character:

To examine this property we compare the $K^- p \to K^-(p\pi\pi)$ data already displayed in Fig. 26 above, to data on $K_L^0 p \to K_S^0(p\pi\pi)$ of approximately the same energy, from the SLAC bubble chamber experiment.[30] The data is selected to isolate out the peripheral $p \to p\pi\pi$ reaction mechanism and the resulting $(p\pi\pi)$ mass spectrum is shown in Fig. 27. The low mass diffractive enhancement in the K^- reaction is not observed in the K_L^0 data, although these two reactions are so very similar. The difference lies in that the K_L^0 and K_S^0 are eigen states of C with opposite sign and therefore the t-channel exchange in the K_L^0 reaction must carry C = -1. This may be viewed as evidence of the C = +1 character of diffractive processes.

(c) Spin-Parity Changes:

As per our "rules" we expect that diffraction will proceed most simply with no change of spin or parity for either the target or projectile particles, but that if there is a change it will

follow the natural spin-parity sequence, viz.

$$P_f = P_i \ (-1)^{\Delta J}$$

This may be thought of as picking up angular momentum in the Pomeron-diffracting-particle scattering.

This is a phenomenological rule, whose main claim to correctness is that there are no known diffractive processes which violate it. There exists rigorous proof for the spin zero case, but there is no general theorem for the more interesting spin situations.

The main evidence for justification for this "rule" is negative in nature (as mentioned above); however, one recent confirmation of the rule comes from a bubble chamber experiment on $\pi^- n \to \pi^- \pi^- p$ at 11.7 GeV/c by the Riverside group.[31] They observe diffractive production of N^*'s decaying into $p\pi^-$ final state. The analysis is free from complications of π-π resonance effects and deals with the well understood two-body elastic decay of the N^*; (i.e. it avoids the complication of previous studies which have observed diffractive production of $N^* \to N\pi\pi$, and then applied assumptions about two-body decays into $\Delta\pi$ final states). The Riverside results show production of P_{11}, D_{13}, F_{15} N^*'s, (i.e. the correct parity sequence for our "rule") and no sign of the D_{15} state. Further, the production phase between the D_{13} and F_{15} processes was found to be 0^o, in agreement with the hypothesis of diffractive production.

On the negative side, three threats to the rule existed last year -- vector K* production by K's, tensor A_2 production by π's and axial vector B production by γ's. Each of these processes violates the natural spin-parity sequence, but claims of "diffraction-like" properties had been made. We discuss them at more length below:

(a) K*(890) Production:

At the Oxford conference data on $K^- p \to K^*_{890} p$ was reported [32] implying that the cross section, which had been falling like p_{lab}^{-2} up to 8 GeV/c actually flattened out to an almost constant value for higher energies. This was taken as evidence of Pomeron contribution to K* production.

However, new data up to 16 GeV/c is now available, [33] and the cross section seems to fall like p_{lab}^{-1} beyond 8 GeV/c and the production and decay characteristics are in good agreement with isoscalar, natural spin parity exchange. Presumably ω^o exchange takes over from π exchange at the higher energies, and this "threat" to the parity rule has disappeared.

(b) A_2 Production:

There have been suggestions for some time that perhaps the A_2 meson is produced via Pomeron exchange, thus violating our simple rule of natural spin-parity excitation in diffraction processes. Kruse, et al. [34] have submitted an analysis of A_2 production in bubble chamber data in the energy range from (5-25) GeV/c. There is also a paper from Ascoli et al. [35] on A_1, A_2, and

A_3 production at 40 GeV/c. The facts are summarized below:

i. The A_2 cross section falls off as $p^{-0.8 \pm 0.08}$ in the (5-25) GeV/c range;

ii. The relative energy dependence of A_1, A_2, and A_3 between 25 GeV/c and 40 GeV/c are essentially the same;

iii. The natural parity exchange contribution to A_2 production falls off as $p^{-0.57 \pm 0.09}$;

iv. The t-channel exchange in A_2 production is mainly isoscalar;

v. The s-dependence of the cross section implies an effective intercept, $\alpha_{eff}(0) \sim 0.7$;

vi. An analysis of the shrinkage of the $J^P = 2^+$ A_2 differential cross section yields an $\alpha_{eff}(0) \sim 0.8$.

The energy dependence and α_{eff} values quoted above are more in agreement with a strong Pomeron contribution to A_2 production than the vector, and tensor meson contributions one expected. However, we must understand at least one other fact before throwing away our current picture of Pomeron processes -- the energy dependence for the A_2 cross section as measured in the $K\bar{K}$ decay mode seems to be faster than $p_{lab}^{-1.0}$. This is a clean reaction in which to study A_2 production with very little background, and the observed momentum dependence is very much in agreement with that expected for meson exchange in the t-channel. Several experiments should be reporting new cross sections for $A_2 \rightarrow K\bar{K}$ within the near future, and we wait impatiently for their results.

(c) Photoproduction of the B-Meson:

Finally, in this section on "bogey-men", we deal with the photoproduction of the B-meson. The reaction $\gamma p \rightarrow Bp$ violates the natural spin-parity series expected in diffractive processes, yet the B signal is observed with the same strength at 2.8, 4.7, and 9.3 GeV.[36] The energy independent cross section has encouraged speculation as to the validity of the simple rules on spin couplings for the Pomeron.

However, the statistics on these observations are rather limited, each energy point having a cross section of $(1.0 \pm 0.4)\mu b$. One could accommodate quite a variety of energy dependences within these measurements. It is an important reaction and to be followed with interest, but the present results are not strong enough to call our ideas on Pomeron coupling to question -- at least not yet.

For the moment the rule seems to be obeyed.

Spin Structure in Diffractive Processes:

Our "rules" assert that diffractive processes are s-channel helicity conserving (SCHC). This hypothesis derives from the early experimental work of the SLAC-Berkeley-Tufts group on their study of ρ^o-meson photoproduction with the polarized photon beam, at 4.7 GeV.[37] They found that the diffractively produced ρ^o-meson maintained the photon helicity in the s-channel. Gilman and coworkers[38] then hypothesized that all diffractive processes

conserved s-channel helicity and showed that the present knowledge of the πN scattering amplitudes was consistent with that assumption.

New data on $\gamma p \to \rho^o p$ at 9 GeV from the S-B-T group[39], and measurements of the R, A parameters in πN[40] and NN[41] scattering by a Saclay group confirm, in the main, the early conclusions. The new experiments are discussed in more detail below.

It is interesting to note that if s-channel helicity conservation really holds, then the old "lore" that the Pomeron behaves in the energy dependence of cross-sections like a particle of spin 1, but has the couplings of a particle of spin 0, cannot be true. SCHC requires quite specific couplings in the t-channel -- in general helicities will flip and there must be quite specific relations between the t-channel spin flip and non-flip couplings.

The density matrix elements from the new S-B-T experiment[39] at 9.3 GeV are shown in Fig. 28. They confirm the dominant behaviour as being SCHC and it holds out to larger t than observed before. However, the ρ_{10} element is quite definitely non-zero as is shown more clearly in Fig. 29. It was confirmed that the effect was real and not due to a scanning bias, by rotating the plane of polarization of the incident photons with respect to the bubble chamber camera axis; no change in the result was found. Further, they find when isolating the separate exchange amplitudes that the effect belongs to the natural-parity exchange amplitude. It is also found that the magnitude of the effect does not change

rapidly with energy. All these factors imply that there is a small helicity flip amplitude, of about 15% the SCHC amplitude, which may be associated with Pomeron exchange. Results of their analysis of the helicity flip contribution are given in Table 9.

The Saclay experiment studied $\pi^{\pm}p$ scattering at 6, 16 GeV/c from a polarized proton target.[40] The recoil proton was detected in a spark chamber polarimeter. The spin rotation parameters R and A were measured. Actually good measurements of R were obtained and A found from the relation $P^2 + A^2 + R^2 = 1$, using the existing precision measurements of the polarization in p-p scattering. Rough measurements of A were taken to resolve the quadratic ambiguity in the above equation. They find A to be close to +1 as expected from SCHC.

At 6 GeV/c, an amplitude analysis was performed using all the available data on total and elastic πN cross sections, differential cross sections, charge exchange cross sections, polarization for elastic and charge exchange reactions and their own new R and A parameters. Results for the isoscalar flip and non-flip amplitudes are shown in Fig. 30. The flip amplitude has a kinematic zero in the forward direction but is certainly non zero at larger t. For the region of $t > 0.2$ GeV^2, they find the ratio of flip to non-flip amplitude to be 0.17 ± 0.2 at 6 GeV/c.

There is not sufficient πN scattering data to perform a complete amplitude analysis at 16 GeV/c but a reasonable choice of solutions gives the same ratio, at 16 GeV/c, to be 0.14 ± 0.03. That is, the πN data shows that SCHC is the dominant amplitude but

that again a small (~ 15%) helicity flip amplitude is present and that it is isoscalar and weakly s-dependent -- presumably associated with the Pomeron. It is important to remember that although the $\gamma \rightarrow \rho$ experiment and this πN experiment are both measuring 15% helicity flip amplitudes which are isoscalar and weakly energy dependent, they are not measuring the same thing; the photon experiment measures the spin structure at the meson vertex while the πN experiment measures the spin structure at the nucleon vertex.

The Saclay group also measured R, A parameters for p-p scattering at 6, 16 GeV/c, and found the parameters consistent with dominance of SCHC. There is not sufficient data to perform an amplitude analysis for p-p scattering, but it is clear that this data would be consistent with a small helicity flip amplitude.

Finally, we must consider the spin structure for inelastic processes. Table 10 summarizes recent work on this question. It shows that the vector meson photoproduction behaves very much like elastic scattering -- SCHC in the main, but with a small helicity violating amplitude. The various diffraction dissociation processes do not conserve s-channel helicity. Most of them are much more close to t-channel helicity conservation, but in general do not conserve that either. Thus, although their inelastic processes looked very much like elastic reactions from the point of view of cross section and differential cross sections, they have very different spin structure. This difference may be due to the fact that these processes are perhaps not really particle production,

but kinematic enhancements, or due to the spin change that occurs in these processes and the complex t-channel spin structure of the Pomeron.

Conclusions:

We have reviewed the data on diffractive reactions and compared them to the set of phenomenological rules developed to describe these processes. In the main, the data agrees with the rules, both for inelastic and elastic reactions. There are, however, some puzzling questions;

- the question of the $\gamma p \rightarrow \phi p$ forward slope as a function of energy,
- the small t structure in p-p scattering,
- the observation of a small helicity flip amplitude associated with the Pomeron,
- the fact that inelastic diffractive dissociation processes do not observe SCHC,
- the exchange mechanism in $\pi p \rightarrow A_2 p$ and its relation to the parity rule,
- the rising p-p total cross sections and what that implies about our definition of asymptopia,
- given that $K^+ p$ and p-p cross sections rise, when will $\pi^{\pm} p$, $\bar{p}p$, γp, etc. start to rise.

All more material for another Moriond.

TABLE 1

The values of the parameters A and n resulting from the fitting of the total cross-section differences above 3 GeV/c to the formula

$$\Delta\sigma = A\, p_{lab}^{-n}.$$

(The errors shown in the table have been evaluated taking into account statistical and systematic errors.)

Cross-section differences	A (mb)	n
$\Delta(\pi^{\mp}p)$	4.0 ± 0.3	0.32 ± 0.02
$\Delta(K^{\mp}p)$	18.1 ± 0.3	0.54 ± 0.02
$\Delta(K^{\mp}n)$	13.0 ± 0.4	0.67 ± 0.02
$\Delta(p^{\mp}p)$	63 ± 2	0.64 ± 0.02
$\Delta(p^{\mp}n)$	49 ± 7	0.61 ± 0.05

TABLE 2

Energy dependence of total and elastic cross section.

$$\sigma \propto p^{-n}$$

Particle	Experiment, n		p Range (GeV/c)
	σ (elastic)	σ (total)	
π^-	(.23 ± .03)	.05 ± .01	(10 - 65)
π^+	(.28 ± .06)	.04 ± .01	(> 10)
K^-	(.39 ± .04)	.07 ± .01	(5 - 55)
K^+	(.09 ± .03)	0 rising slowly	(5 - 20) (20 - 60)
$\bar{p}$	.46 ± .02)	.11 ± .01	(10 - 50)
p	(.26 ± .02)	.03 ± .01	(10 - 30)

TABLE 3

Ratios

σ_{el} and σ_{tot}

	p_{lab} (GeV/c)	Ratio
π^-	5.5	.188 ± .005
	55.0	.138 ± .007
π^+	7.7	.192 ± .004
	16.0	.170 ± .006
K^-	10	.140 ± .003
	40	.126 ± .014
K^+	5	.225 ± .024
	15	.196 ± .017
p	6	.294 ± .006
	60	.187 ± .008
	200	.174 ± .005
	1000	.176 ± .007
$\bar{p}$	8.0	.225 ± .012
	16.0	.185 ± .010
	40.0	.178 ± .018

TABLE 4

RATIO OF $\frac{\sigma(xp \to xp)}{\sigma(\bar{x}p \to \bar{x}p)}$

	σ_{el}(mb)	p_{lab}	
K^-	3.15 ± .08	(10 GeV/c)	.94 ± .09
	2.60 ± .3	(40 GeV/c)	
K^+	3.34 ± .3	(10 GeV/c)	
π^-	4.8 ± .1	(10 GeV/c	1.00 ± .02
π^+	4.8 ± .1	(10 GeV/c)	
$\bar{p}$	13.9 ± .3	(10 GeV/c)	1.05 ± .11
	8.0 ± .8	(40 GeV/c)	
p	11.7 ± .2	(10 GeV/c)	
	7.6 ± .3	(40 GeV/c)	

TABLE 5

Energy Dependence of Diffraction Process,
$\sigma \propto p^{-n}$ ((5-20) GeV)

Process	n
$K^o \rightarrow Q^o$	0.59 ± 0.16
$K^+ \rightarrow Q^+$	0.60 ± 0.05
$\pi^- \rightarrow A_1^-$	0.41 ± 0.11
$N \rightarrow N\pi\pi$	0.4 ± 0.6
$\pi^- \rightarrow A_3^-$	0.8 ± 0.3

For comparison, the elastic scattering energy dependence is:

Process	n
K^+p	0.09 ± 0.03
K^-p	0.39 ± 0.04
πN	~ 0.2
NN	~ 0.2

TABLE 6

Process		Slope (GeV^{-2})
$\gamma \rightarrow \rho$	~	6-8
$\pi \rightarrow A_1$	~	9-11
$\pi \rightarrow A_3$	~	8
$K \rightarrow Q$	~	5-7
$\bar{K} \rightarrow \bar{Q}$	~	8-10
$N \rightarrow (N\pi\pi)_{1400}$	~	10-11
$N \rightarrow (N\pi\pi)_{1700}$	~	5

For comparison, the elastic slopes are ~

Process		Slope (GeV^{-2})
γN	~	6
πN	~	7-9
KN	~	5-6
$\bar{K}N$	~	7-8
NN	~	9-10

Factorization Test in πN and pp Reactions

$R_1 = \frac{\sigma(\pi^- p \to \pi^- p)}{\sigma(pp \to pp)} = 0.43$
$R_2 = \frac{\sigma(\pi p \to \pi(p\pi^0))}{\sigma(pp \to p(p\pi))} = 0.46 \pm .15$
$R_3 = \frac{\sigma(\pi p \to \pi(p\pi^+\pi^-))}{\sigma(pp \to p(p\pi^+\pi^-))} = 0.35 \pm .18$
$R_4 = \frac{\sigma(\pi p \to \pi(p\pi\pi\pi)}{\sigma(pp \to p(p\pi\pi\pi))} = 0.45 \pm .15$

TABLE 8

A Factorization Test for γp , πp, and pp Reactions

	Momentum (GeV/c)		
	(6-10)	(10-14)	(14-18)
$R_1 = \frac{\sigma(\gamma p \to \rho^0 p)}{\sigma(\gamma p \to \rho^0 p\pi^+\pi^-)}$	0.053 ± 0.014	0.035 ± 0.014	0.055 ± 0.024
$R_2 = \frac{\sigma(pp \to pp)}{\sigma(pp \to pp\pi^+\pi^-)}$	0.064 ± 0.07	0.061 ± .008	0.060 ± 0.009
$R_3^+ = \frac{\sigma(\pi^+ p \to \pi^+ p}{\sigma(\pi^+ p \to \pi^+ p\pi^+\pi^-)}$		0.061 ± .006	0.063 ± 0.003
$R_3^- = \frac{\sigma(\pi^- p \to \pi^- p)}{\sigma(\pi^- p \to \pi^- p\ \pi^+\pi^-)}$		0.052 ± 0.005	0.059 ± 0.003

TABLE IX

s-CHANNEL HELICITY-FLIP AMPLITUDE RATIOS IN THIS EXPERIMENT AND IN πN SCATTERING[6] FOR $.18 < |t| < .80$ GeV^2

Amplitude Ratios*	Experimental Values of Density Matrix Elements			
	2.8 GeV	4.7 GeV	9.3 GeV	Average
Photoproduction				
$\lvert T_{01}\rvert^2/\lvert T_{11}\rvert^2 \simeq \rho^0_{00}$	-.01±.03	.07±.02	-.01±.02	.018±.012
$\lvert T_{-11}\rvert^2/\lvert T_{11}\rvert^2 \simeq \rho^1_{1-1} + \mathrm{Im}\,\rho^2_{1-1}$	.04±.05	.11±.05	-.02±.05	.04±.03
$\mathrm{Im}\,T_{01}/\lvert T_{11}\rvert \simeq 2\,\mathrm{Re}\,\rho^0_{10}$	.16±.03	.12±.03	.14±.02	.14±.016
$\mathrm{Im}\,T_{-11}/\lvert T_{11}\rvert \simeq \rho^0_{1-1}$	-.06±.03	-.05±.03	-.10±.02	-.08±.02
πN Scattering				
$\lvert F^0_{+-}\rvert/\lvert F^0_{++}\rvert$ Isospin 0 Exchange		6 GeV/c		.15±.02

*The nucleon helicities in the photoproduction amplitudes listed are $\frac{1}{2}\frac{1}{2}$ (or $-\frac{1}{2}-\frac{1}{2}$).

Table X

Reaction	P_{lab} (GeV/c)	Group	Paper	Analyzer	SCHC	TCHC
$\gamma \to \rho^0$	2.8, 4.7, 9.3	Ballam et al.	307, 411	Azimuthal and polar angle of π.	Yes (They report a possible 2% flip contribution.)	No
	(2.7 - 4.0)	Gladding et al.	206	Same	Yes ($t < .5$ GeV)	No
	(4 - 6)	Struczinski et al.	325	Same	Yes	No
	(9 - 16)	Bulos et al.	349	Same	Yes	No
$\gamma \to \omega$	2.8, 4.7, 7.3	Ballam et al.	411	Same	Yes	No
$\gamma \to \phi$	2.8, 4.7, 7.3	Ballam et al.	411	Same	Consistent	No
$\pi \to A_1$ $\pm$	8.16	ABBCH	390	LPS selection, and polar angle of π.	No	No
$\pm$	16	ABBCCHLVW	169	Azimuthal study, normal to 3π and polar angle of π.	No	No
-	40	Antipov et al.	442		No	Slight Violation
-	4.5	Beketov et al.	833	Normal to 3π plane.	No	Yes
$\pi^- \to A_3^-$	(5 - 2.5)	Ascoli et al.	341	π^+ polar angle	No	Yes (but not very strong)
$K \to Q$ -	10	ABBCCHLVW	169	Azimuthal study, and normal to plane and π polar angles.	No	No
-	14.3	Barloutaud et al.	371	Normal to $K\pi\pi$ plane, and polar angles of π.	No	No
0	(4 - 12)	Brandenburg et al	347	Normal to $K\pi\pi$ plane.	No	Yes (but not very strong)
1400	10, 16	ABBCCHLVW	169	Azimuthal study, and normal, and polar.	Data Insensitive	
1700	10, 16	ABBCCHLVW	169	Same	No	Yes
$p \to p\pi\pi$ All	8, 16	ABBCH	390	LPS and polar angles of π.	No	Yes
All	25	Chapman et al.	452	Azimuthal	No	No
1600	11.6	Oh et al.	260		No	Yes

Figure Captions

1. Differential elastic scattering cross-section for 64 MeV α-particles on Fe^{58}, divided by the Rutherford scattering cross-section, as a function of the C of M scattering angle.
2. Energy dependence of the total cross-sections of $\pi^{\pm}$, $K^{\pm}$, $p^{\pm}$ in hydrogen.
3. Energy dependence of the total p-p cross-section through the Serpukov, NAL and ISR energy regions.
4. Energy dependence of the p-p elastic cross-section.
5. Energy dependence of $\pi^{-}p$, $K^{-}p$ and $\bar{p}p$ elastic cross-sections.
6. The ratio of elastic to total p-p cross-sections as a function of energy.
7. Differential cross section for elastic p-p scattering at the CERN ISR.
8. Energy dependence of the slope of the elastic p-p differential cross-section, for two regions of t--(a) $t < 0.1$ GeV^2, (b) $0.15 \leq t \leq 0.5$ GeV^2.
9. Differential cross-section for elastic $\pi^{-}p$, $K^{-}p$ and $\bar{p}p$ scattering at 25 and 40 GeV/c.
10. Energy dependence of the slope of elastic $\pi^{\pm}$, $K^{\pm}$, $p^{\pm}$ scattering in hydrogen.
11. Energy dependence of the cross-section for the process $K_L^o p \rightarrow K_S^o \pi^+ \pi^- p$, and the sub-process $K_L^o p \rightarrow Q^o p$.
12. Differential cross-section for elastic $K^{\pm}p$ scattering at 13 GeV/c.

13. Differential cross-sections for $K^o p \rightarrow Q^o p$ (squares) and $\overline{K}^o p \rightarrow \overline{Q}^o p$ (circles) over the momentum range (4-12) GeV/c.

14. Energy dependence of the slope parameter of the Pomeron contribution in--$K^+ p$ scattering shown as the shaded region, and $\pi^{\pm} p$ scattering, shown as the circles.

15. Fits to the differential cross-section of ρ^o photo-production to the sum of P and f exchange utilising Dual Absorption Model. The energy dependence of the slope parameter for the P contribution to the process is also shown.

16. Energy dependence of the cross-section for the reaction $\gamma p \rightarrow \phi p$.

17. Differential cross-section for $\gamma p \rightarrow \phi p$ at several energies.

18. The slope of the differential cross-section for $\gamma p \rightarrow \phi p$ as a function of energy.

19. The s-dependence of the differential cross-section for $\gamma p \rightarrow \phi p$ at a momentum transfer, $t = 0.6$ GeV^2. The data indicate no shrinkage of the ϕ cross-section at this value of t.

20. Differential cross-section for elastic p-p scattering at several energies, showing strong shrinkage at all values of t.

21. Schematic diagrams for elastic π^-, K^-, and $\overline{p}$ scattering and diffractive production of N*(1690).

22. Ratio of elastic cross-section to the N*(1690) production cross-section for incident π^-, K^- and $\overline{p}$ at 8, 16 GeV/c, as a function of momentum transfer.

23. A schematic of diffractive reactions studied in a test of

factorization. The ratios R_1-R_4 refer to the ratio of the cross-sections of reactions when the top two vertices (pion and proton elastic scattering) are joined successively to the bottom four vertices representing proton diffraction into a proton plus zero, one, two or three pions respectively.

e.g. $R_1 = \left[\frac{\sigma(\pi p \rightarrow \pi p)}{\sigma(pp \rightarrow pp)}\right]$

$R_2 = \left[\frac{\sigma(\pi p \rightarrow \pi p\pi)}{\sigma(pp \rightarrow pp\pi)}\right]$

etc.

24. A schematic of diffractive reactions studied in a test of factorisation. The ratio R_1, R_2, R_3 refers to the ratio of the cross-sections when each of the upper vertices ($\gamma \rightarrow \rho$, $p \rightarrow p$, $\pi \rightarrow \pi$) is connected with the two lower vertices, representing proton diffraction into a proton or a ($p\pi\pi$) system, respectively.

e.g. $R_1 = \left[\frac{\sigma(\gamma p \rightarrow \rho p)}{\sigma(\gamma p \rightarrow \rho p\pi\pi)}\right]$

$R_2 = \left[\frac{\sigma(pp \rightarrow pp)}{\sigma(pp \rightarrow pp\pi\pi)}\right]$

$R_3 = \left[\frac{\sigma(\pi p \rightarrow \pi p)}{\sigma(\pi p \rightarrow \pi p\pi\pi)}\right]$

25. Mass spectrum for ($N\pi$) in $\pi N \rightarrow \pi\pi N$ at 16 GeV/c.

26. Mass spectrum for ($N\pi\pi$) in $\bar{K}N \rightarrow \bar{K}(N\pi\pi)$ at 10 GeV/c.

27. Mass spectrum for ($N\pi\pi$) in $\bar{K}N \rightarrow \bar{K}(N\pi\pi)$ collissions--10 GeV/c K^- and (6-12) GeV/c K^0_L.

28. Density matrix elements for ρ^0 photo-production by polarised

photons at 9.3 GeV.

29. The momentum transfer dependence of the matrix element, ρ_{10}, at 2.8, 4.7 and 9.3 GeV. This matrix element indicates the presence of a spin flip amplitude.

30. The momentum transfer dependence of the flip and non flip isoscalar πN scattering amplitudes at 6 GeV/c.

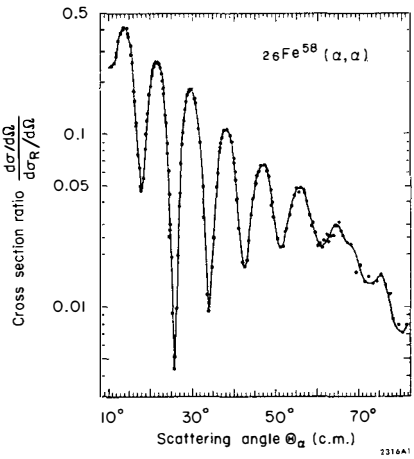

Figure 1

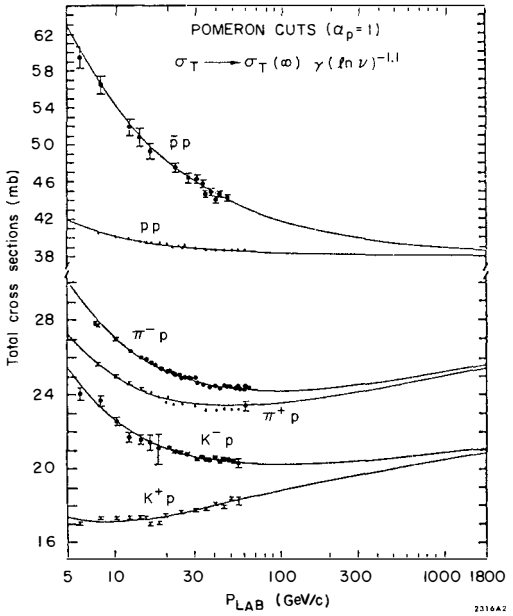

Figure 2

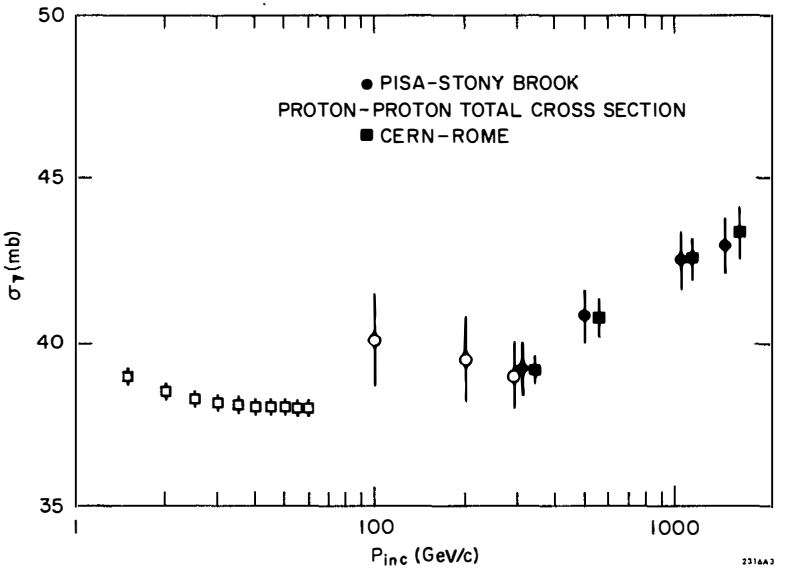

Figure 3

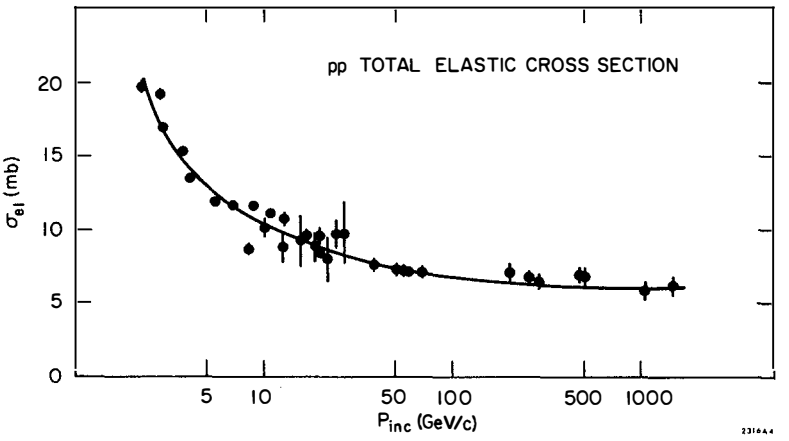

Figure 4

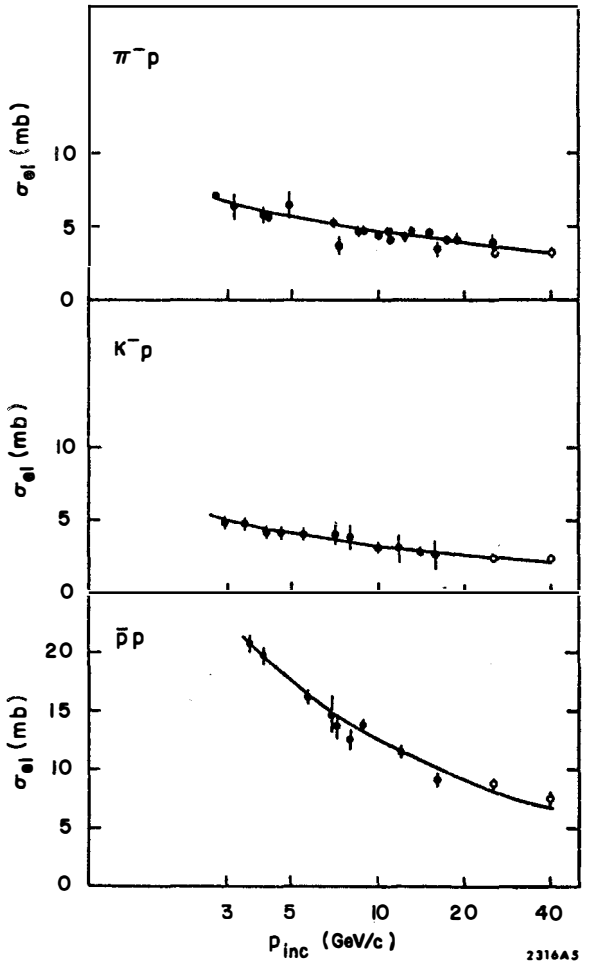

Figure 5

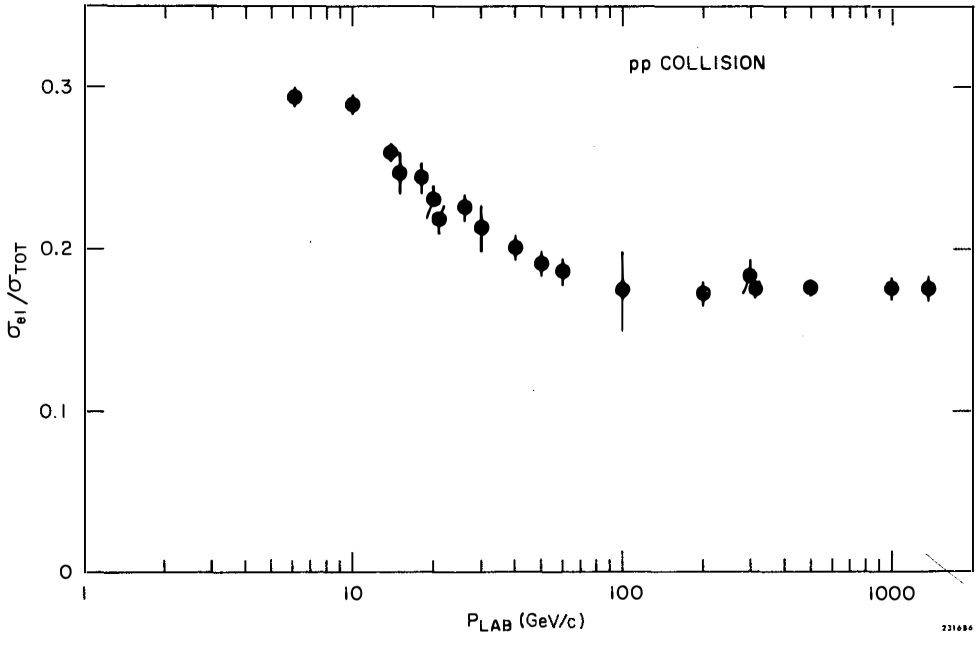
pp COLLISION
0.3
0.2
0.1
0
σ_{el}/σ_{TOT}
1
10
100
1000
P_{LAB} (GeV/c)
231686

Figure 6

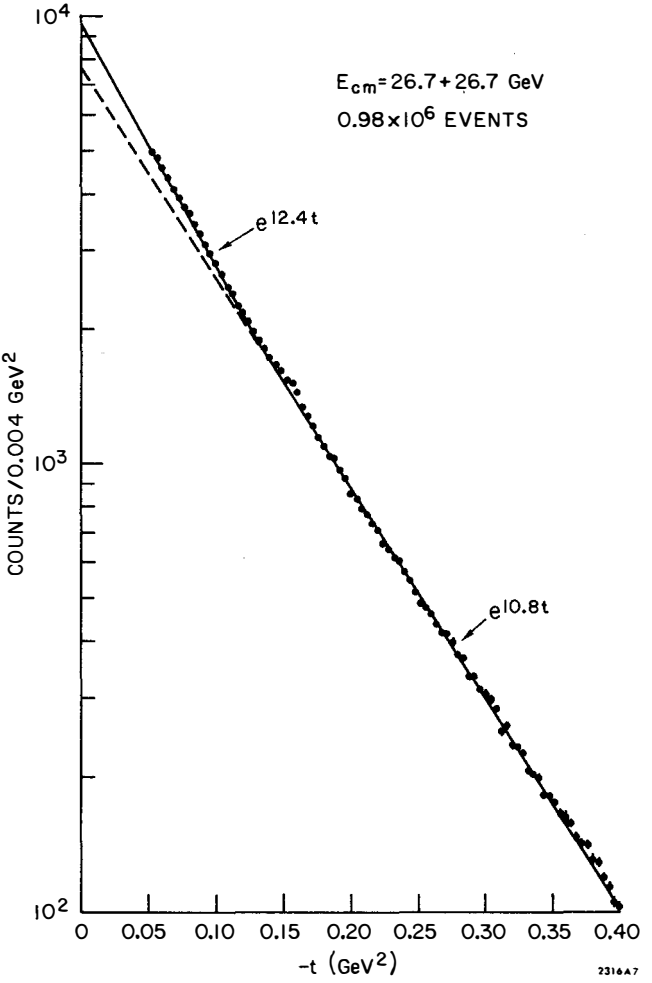
10^4
10^3
10^2
E_{cm}=26.7+26.7 GeV
0.98×10^6 EVENTS
$e^{12.4t}$
$e^{10.8t}$
COUNTS/0.004 GeV^2
0
0.05
0.10
0.15
0.20
0.25
0.30
0.35
0.40
-t (GeV^2)
2316A7

Figure 7

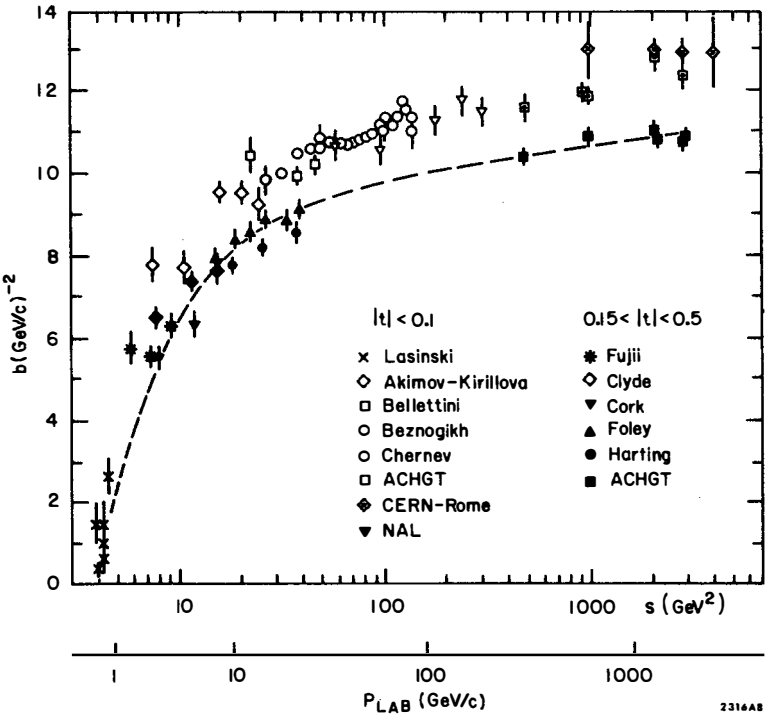
b (GeV/c)$^{-2}$
14
12
10
8
6
4
2
0
|t| < 0.1
0.15< |t|<0.5
Lasinski
Akimov-Kirillova
Bellettini
Beznogikh
Chernev
ACHGT
CERN-Rome
NAL
Fujii
Clyde
Cork
Foley
Harting
ACHGT
10
100
1000
s (GeV^2)
1
10
100
1000
P_{LAB} (GeV/c)
2316A8

Figure 8

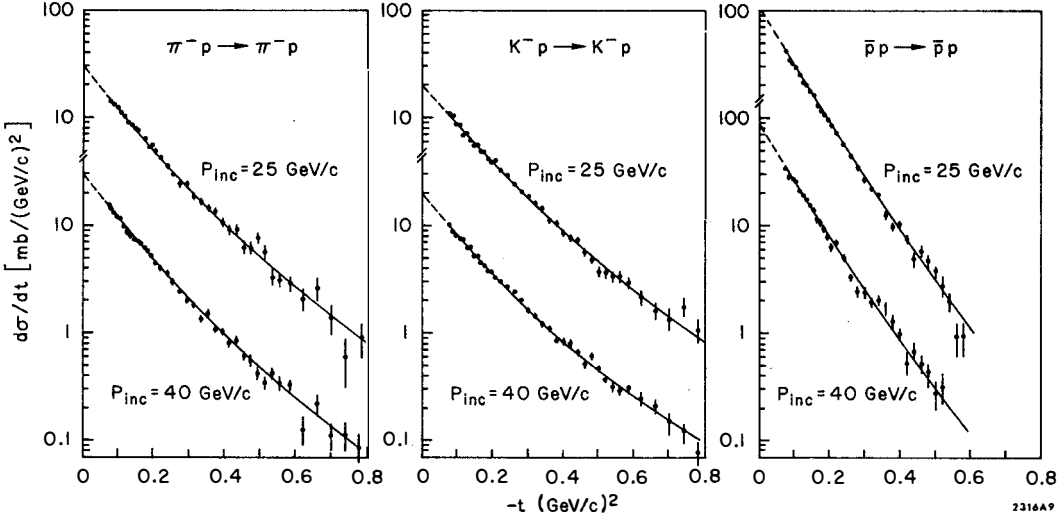
$\pi^- p \rightarrow \pi^- p$
$K^- p \rightarrow K^- p$
$\bar{p} p \rightarrow \bar{p} p$
$P_{inc} = 25$ GeV/c
$P_{inc} = 40$ GeV/c
$d\sigma/dt$ [mb/(GeV/c)^2]
$-t$ (GeV/c)^2
100
10
1
0.1
0
0.2
0.4
0.6
0.8
2316A9

Figure 9

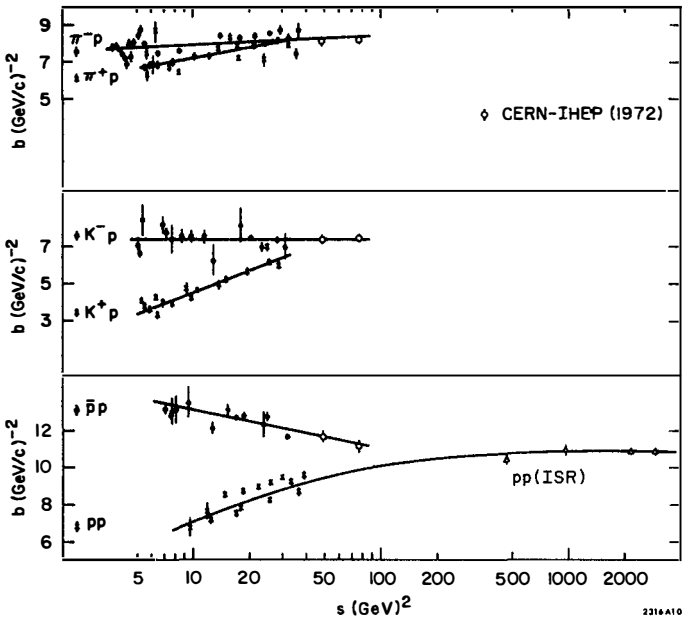

Figure 10

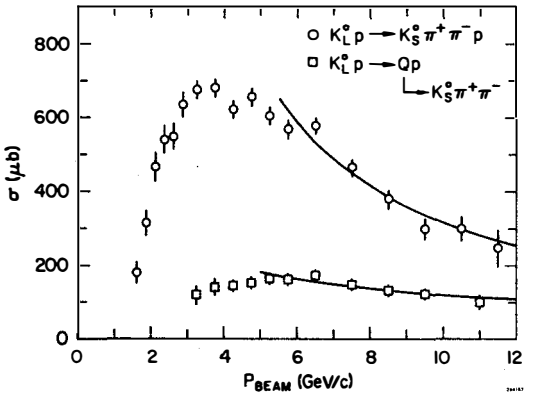

Figure 11

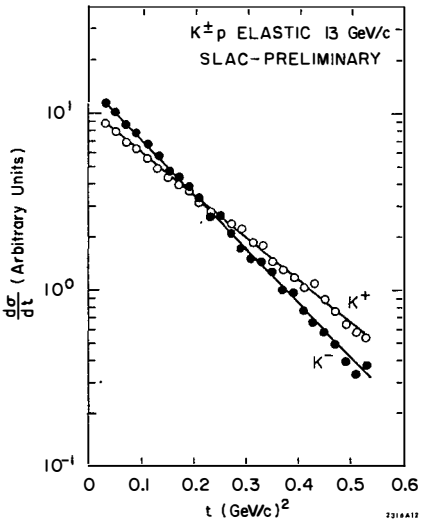

Figure 12

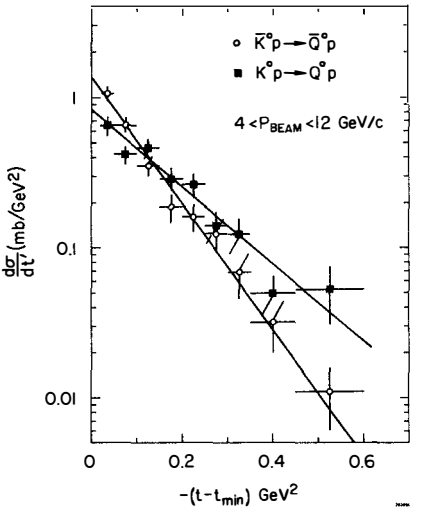

Figure 13

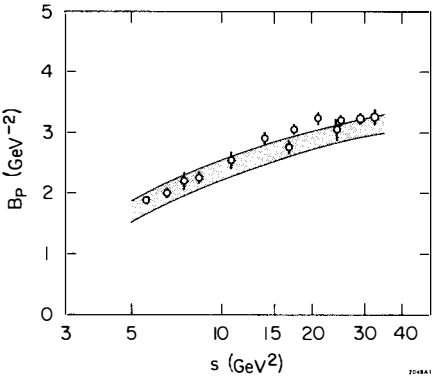

Figure 14

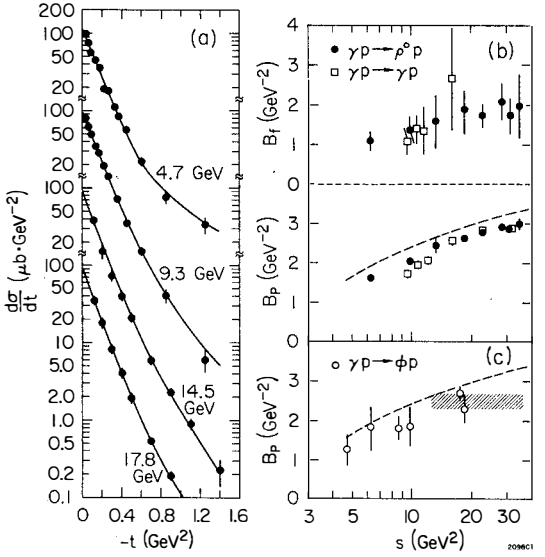

Figure 15

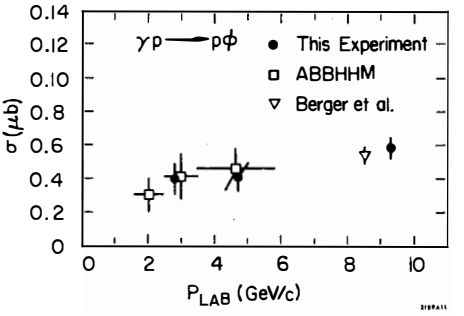
0.14
0.12
0.10
0.8
0.6
0.4
0.2
0
σ(μb)
γp → pφ
This Experiment
ABBHHM
Berger et al.
0
2
4
6
8
10
P_LAB (GeV/c)

Figure 16

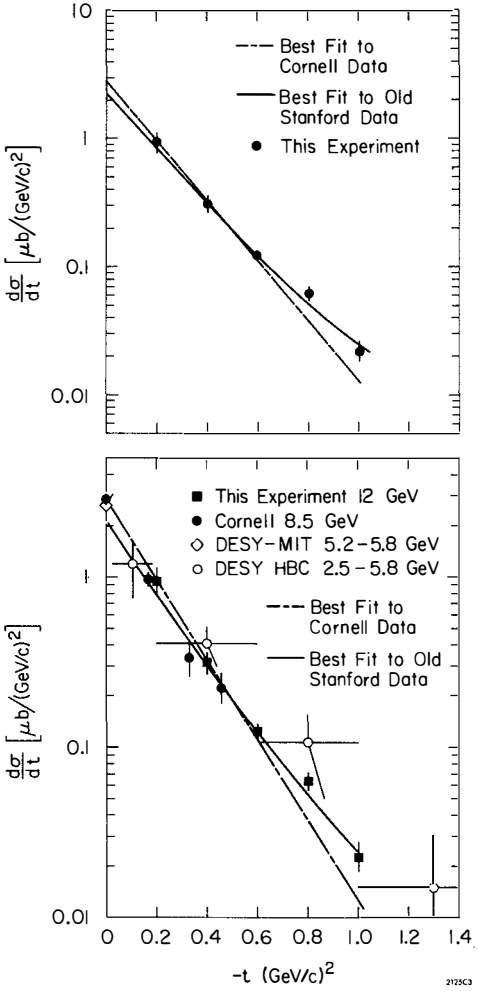
10
1
0.1
0.01
dσ/dt [μb/(GeV/c)²]
Best Fit to Cornell Data
Best Fit to Old Stanford Data
This Experiment
This Experiment 12 GeV
Cornell 8.5 GeV
DESY-MIT 5.2-5.8 GeV
DESY HBC 2.5-5.8 GeV
Best Fit to Cornell Data
Best Fit to Old Stanford Data
0
0.2
0.4
0.6
0.8
1.0
1.2
1.4
-t (GeV/c)²
2125C3

Figure 17

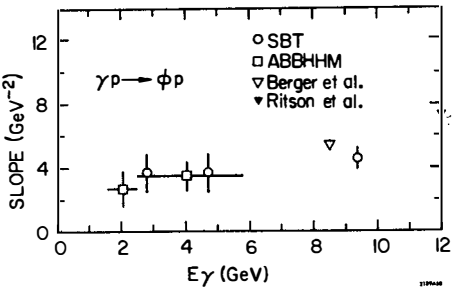

Figure 18

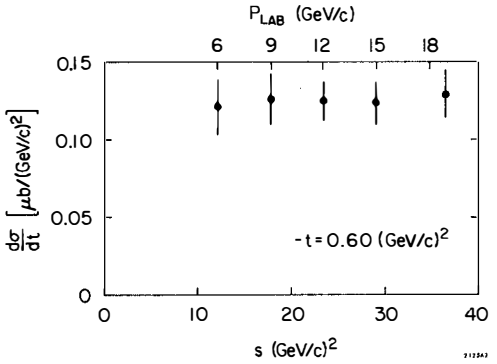

Figure 19

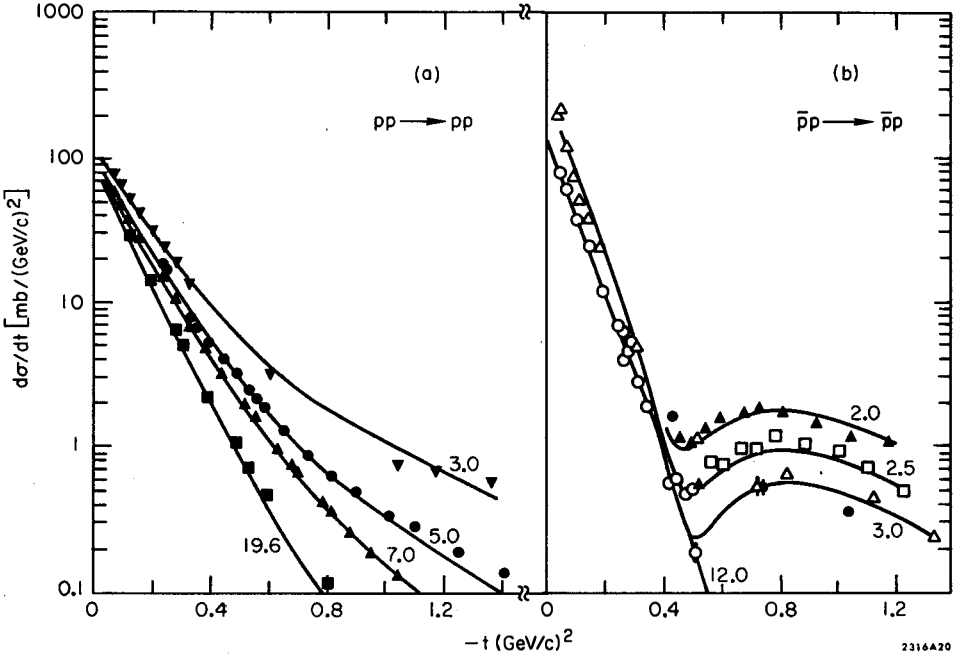
1000
100
10
1
0.1
dσ/dt [mb/(GeV/c)²]
(a)
pp → pp
3.0
5.0
7.0
19.6
0
0.4
0.8
1.2
(b)
p̄p → p̄p
2.0
2.5
3.0
12.0
0
0.4
0.8
1.2
−t (GeV/c)²
2316A20

Figure 20

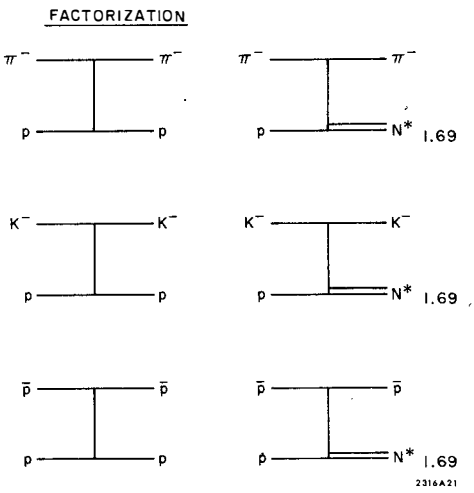

Figure 21

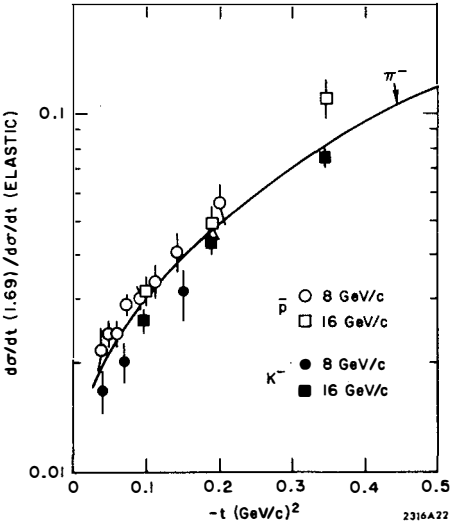

Figure 22

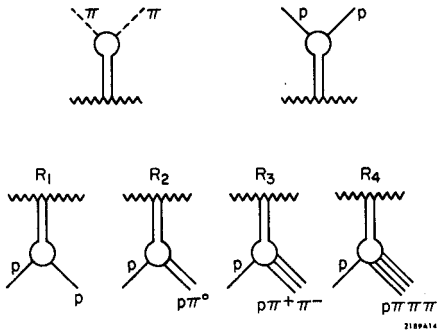

Figure 23

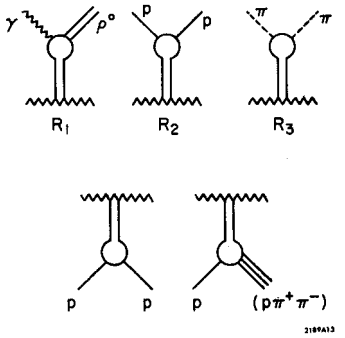

Figure 24

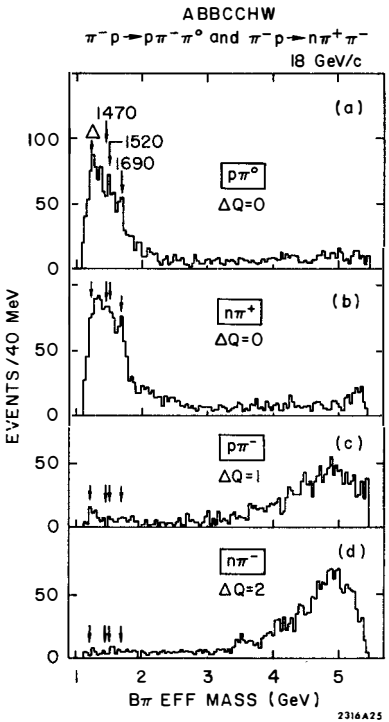

Figure 25

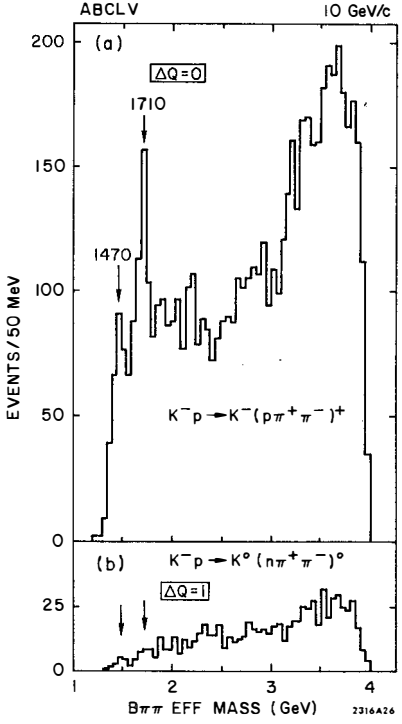

Figure 26

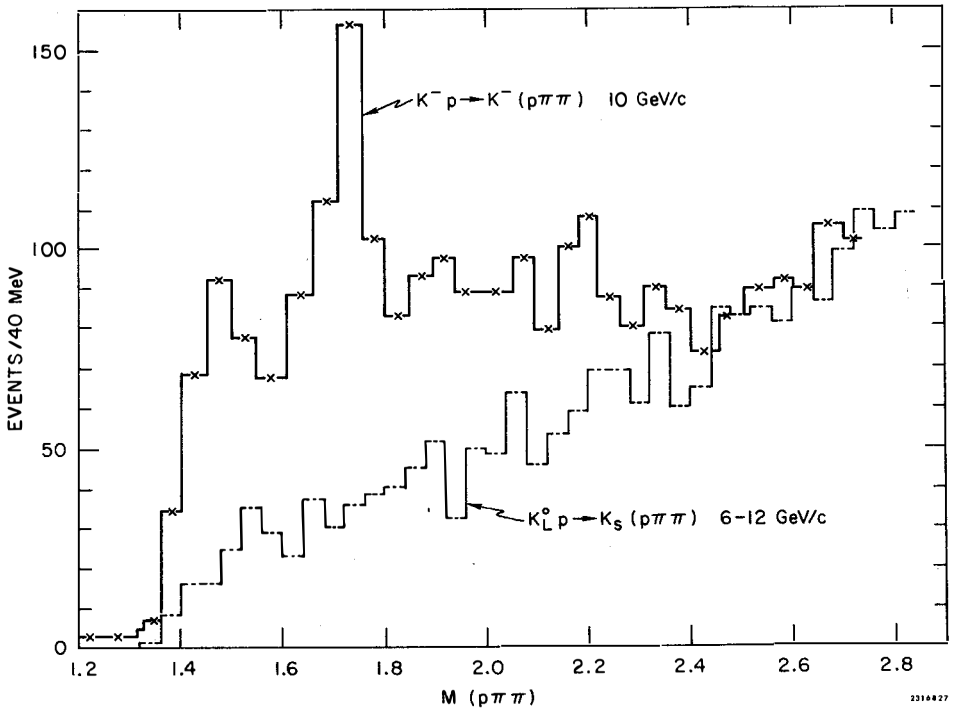
150
100
50
0
EVENTS/40 MeV
$K^- p \to K^- (p\pi\pi)$ 10 GeV/c
$K^0_L p \to K_S (p\pi\pi)$ 6-12 GeV/c
1.2
1.4
1.6
1.8
2.0
2.2
2.4
2.6
2.8
M $(p\pi\pi)$
2316827

Figure 27

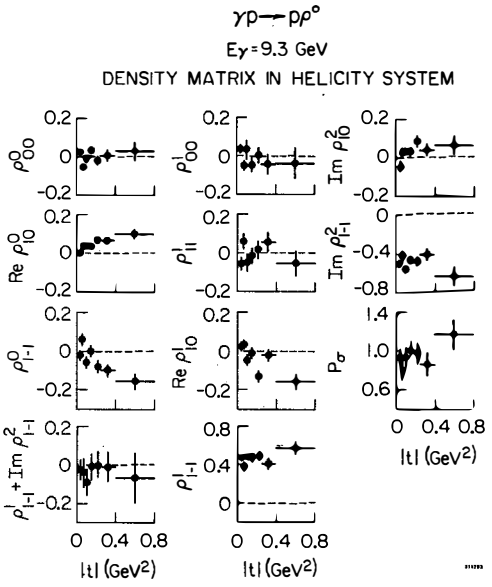
γp→pρ°
Eγ=9.3 GeV
DENSITY MATRIX IN HELICITY SYSTEM
ρ^0_{00}
ρ^1_{00}
Im ρ^2_{10}
Re ρ^0_{10}
ρ^1_{11}
Im ρ^2_{1-1}
ρ^0_{1-1}
Re ρ^1_{10}
P_σ
$\rho^1_{1-1}+\mathrm{Im}\,\rho^2_{1-1}$
ρ^1_{1-1}
0.2
0
-0.2
0.8
0.4
-0.4
-0.8
1.4
1.0
0.6
0 0.4 0.8
|t| (GeV²)

Figure 28

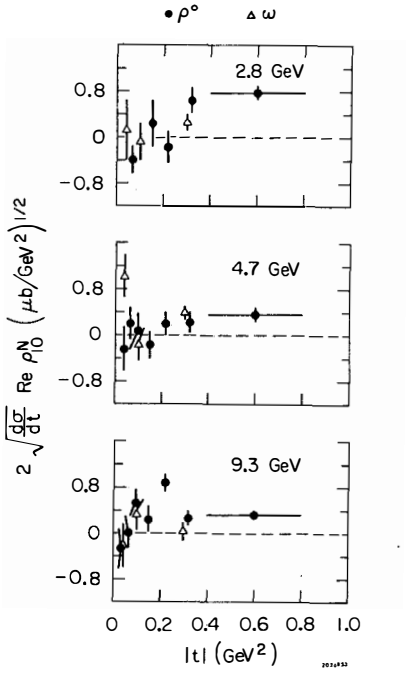

Figure 29

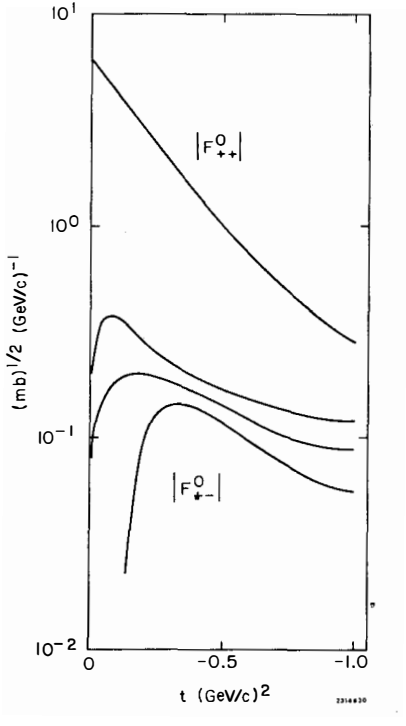

Figure 30

REFERENCES

1. F. K. McGowan, W. T. Milner, and H. J. Kim, ORNL-CPX-1, Charged Particle Cross Section Center, Oak Ridge National Lab., Oak Ridge.

2. M. L. Good and W. D. Walker, Phys. Rev. 120, 1854 (1960).

3. G. Giacomelli, XVI International Conference on High Energy Physics, Chicago-Batavia 1972 Proceedings, p. 219, Vol. 3 (1972).

4. S. P. Denisov, et al., Paper submitted to XVI International Conference on High Energy Physics, Chicago-Batavia, 1972.

5. V. V. Akiviov et al., Proceedings of 11th International Conference on Cosmic Rays, Budapest 1969.

6. S. R. Amendolia et al., submitted to Phys. Letters

7. U. Amaldi et al., submitted to Phys. Letters

8. G. G. Beznogikh et al., Paper submitted to XVI International Conference on High Energy Physics, Chicago-Batavia 1972.

9. Yu M. Antipov et al., Paper submitted to XVI International Conference on High Energy Physics, Chicago-Batavia 1972.

10. G. Barbiellini et al., Phys. Letters B39, 663 (1972), and Phys. Letters B35, 355 (1971).

11. G. Giacomelli, Rapporteur's talk at XVI International Conference on High Energy Physics, Chicago-Batavia, 1972.

12. E. Leader and M. R. Pennington, Phys. Rev. Letters 27, 1325 (1971).

13. D. W. G. S. Leith, Review talk at XVI International Conference on High Energy Physics, Chicago-Batavia 1972.

14. G. Brandenburg et al., SLAC PUB 1038 (1972).

15. ABBCH Collaboration, Paper submitted to XVI International Conference on High Energy Physics, Chicago-Batavia, 1972.

16. J. Ballam, et al., SLAC PUB 900; P. Baillon et al., Paper submitted to XVI International Conference on High Energy Physics, Chicago-Batavia, 1972.

17. R. K. Carnegie et al., Paper submitted to XVI International Conference on High Energy Physics, Chicago-Batavia, 1972.

18. M.Davier, Phys. Letters 40B, 369 (1972).

19. G. Chadwick et al., SLAC PUB 1093.

20. R. Anderson et al., SLAC PUB 1086.

21. D. R. O. Morrison, Rapporteur talk at Lund International Conference, 1969.

22. R. Anderson et al., SLAC PUB 1085.

23. J. Ballam et al., Paper submitted to XVI International Conference on High Energy Physics, Chicago-Batavia, 1972.

24. H. Alvensleben et al., Paper submitted to XVI International Conference on High Energy Physics, Chicago-Batavia, 1972.

25. H. Alvensleben et al., Paper submitted to XVI International Conference on High Energy Physics, Chicago-Batavia, 1972.

26. D. R. O. Morrison, Rapporteur talk at Kiev International Conference on High Energy Physics, Kiev, U.S.S.R. 1971.

27. S. Ljung et al., Paper submitted to XVI Internation al Conference on High Energy Physics, Chicago-Batavia, 1972.

28. W. Kittel, S. Ratti, and L. Van Hove, Nucl.Phys. B30, 333, (1971).

29. F. Liu et al., SLAC PUB 1047.

30. G. Brandenburg et al., private communication.

31. Y. Oh et al., Paper submitted to XVI International Conference on High Energy Physics, Chicago-Batavia, 1972.

32. R. Barloutaud, Rapporteur talk at the Oxford International Conference, 1971.

33. Y. Goldschmidt-Clermont, Review talk at the XVI International Conference on High Energy Physics, Chicago-Batavia, 1972.

34. U. Kruse et al., Paper submitted to XVI International Conference on High Energy Physics, Chicago-Batavia, 1972.

35. G. Ascoli et al., Paper submitted to XVI International Conference on High Energy Physics, Chicago-Batavia, 1972.

36. J. Ballam et al., Contribution to Cornell International Conference on Electron and Photon Interactions at High Energies, 1969.

37. J. Ballam et al., Phys. Rev. Letters 24, 960, 1970.

38. F. Gilman et al., Phys. Letters 31B, 387, 1970.

39. J. Ballam et al., SLAC PUB 1092.

40. A. de Lesquer et al., Phys. Letters 40B, 277, (1972); G. Cozzika et al., Phys. Letters 40B, 281 (1972).

41. J. Deregel et al., Paper submitted to XVI International Conference on High Energy Physics, Chicago-Batavia, 1972.